Preliminary Experimental Study of Propulsive Performance of Hollow Rocket Rotating Detonation Engines with Designed Laval Nozzle

Yunzhen Zhang, Zhuang Ma, Jianping Wang
Center for Combustion and Propulsion, CAPT & SKLTCS, Dept. Mechanics and Engineering Sciences, College of Engineering, Peking University
Beijing, 100871, China

Shujie Zhang
Beijing Istitute of Astrnautical Systems Engineering
Beijing, 100076, China

1 Introduction

The rotating detonation engine (RDE) is a typical type of the detonative propulsion system and has drawn particular interests nowadays because of its several advantages. The early attempts to achieve rotating detonation waves (or spinning detonation waves) were conducted by Voitsekhovskii[1] and Nicholls[2]. Ever since Bykovskii achieved steady rotating detonation on experiments once again and carried out a series of experiments[3], the RDE has returned back to our sights and has drawn more and more attentions.

The rotating detonation waves of RDE mostly run in an annular chamber. The hollow chamber that has no inner cylinder, in the meantime, is another major configuration of combustion chamber, which was first proposed by Tang et al[4]. Tang[4] firstly verified the feasibility of this kind of chamber numerically, and then Lin[5], Anand[6] et al. verified it in experiments. Zhang[7] et al. have carried out some experiments in the hollow chamber with Laval nozzle attached, but what they concerned about is the stability of RDE's operation and its similarity to the tangential instability in the traditional rocket, and they didn't pay attention to the propulsive performance of their combustors. However, researchers from Nagoya University have done plenty of experiments to investigate the propulsive performance of RDE with hollow chamber. Kawasaki[8] investigated the effects annular width has on RDE. Experiments of nozzleless combustors with 0,9,15,23,31mm annular width were conducted and it led to the result that the thrust would decrease as the annular width become larger. But as there are no nozzle attached to the chamber, the exit area of the combustor wasn't kept constant as the annular width varied, which means the data they collected couldn't represent the real potential of the propulsive performance. Goto[9] and Yokoo[10] investigated the propulsive performance of a nozzleless RDE of small scale (20 mm diameter of the combustion chamber) and got relatively high performance. But as there were no nozzle attached, the role of the nozzle in the operation of RDE still remains unclear.

In this study, we performed a preliminary research to investigate the propulsive performance of hollow RDE of normal scale with Laval nozzle.

2 Experiment System and Description

The experiment object we used in this study is a combustor of RDE with a hollow combustion chamber. The schematic of this combustor is shown in Figure 1. The Fuel and the oxidizer are feed into the combustion chamber through an array of 90 groups of coaxial injecting tubes, which are evenly distributed in one circle. Each coaxial tube contains an inner tube and an outer hole. The material of the inner tube is 304 stainless steel. The inner diameter and the wall thickness of the inner tube are 1 mm, 0.2 mm, respectively. The diameter of the outer hole of the coaxial tube is 2.2 mm. During the engine operation, the fuel is injected into the chamber through the inner tubes of the coaxial injectors, and the oxidizer is injected into the chamber through the outer holes of the coaxial injectors. The thrust chamber is a hollow chamber with no inner cylinder. The diameter of the chamber is 120 mm, and the total length of the straight section of the chamber is 175 mm. After the thrust chamber, there is a designed Laval nozzle attached to the chamber. Assuming isentropic expansion, and calculating from our previous experiment data, we choose two sets of diagrams of the throat and the exit, which are shown in Table 1, and so the contraction ratio can be determined $\varepsilon = A_c/A_t$.

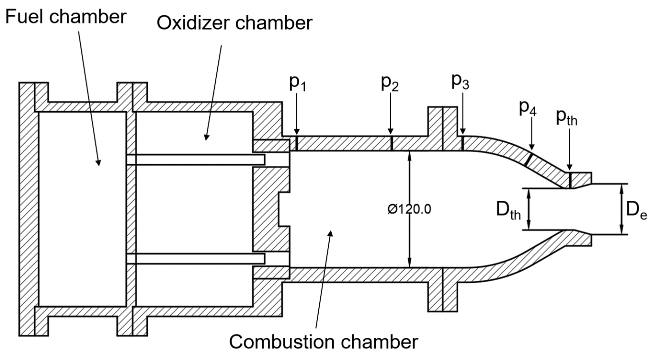

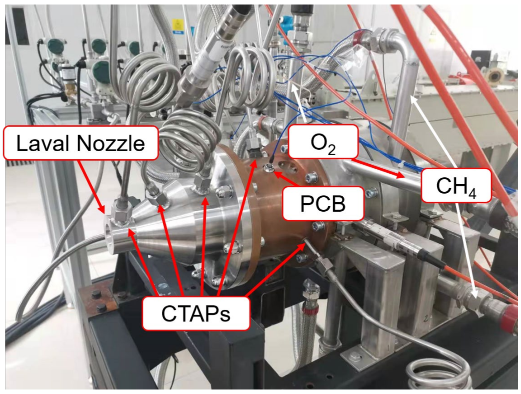

Figure 1: The schematic diagram and the picture of the hollow RDE in the study

Table 1: RDE geometry dimensions

Part	Geometry measured	dimension	
Injeting holes	Inner tube diameter	1.0 mm	
	Inner tube wall thickness	0.2 mm	
	Outer hole diameter	2.2 mm	
	Number (cycles × holes)	1 × 90	
Thrust chamber	Diameter	120 mm	
	Length	175 mm	
Laval nozzle		Nozzle.1	Nozzle.2
	Throat diameter D_{th}	30.8 mm	43 mm
	Contraction ratio ε	0.066	0.128
	Exit diameter D_e	40.8 mm	55 mm
	Diatraction area ratio	1.75	1.64

Three CTAPs are attached to the combustor to measure the low frequency average pressure of different portions. The first CTAP's portion is just 2 mm away from the thrust wall. The flow here is very weak and the fresh gas has just been injected into the chamber which hasn't been detonated yet, so the low frequency pressure p_1 measured here can be regarded as the total pressure just after injection. The CTAP which measures the p_3 is located at the entrance of the Laval nozzle. The CTAP which measures p_{th} is located at the throat of the Laval nozzle. Our previous numerical study has shown that the non-stationarity caused by the periodic rotating detonation has become very weak at the end of the thrust chamber. Accordingly, and under the assumption of isentropic expansion, we can estimate the total pressure after detonation when it is choked at the throat :

$$p_0 = p_{\mathrm{th}}\left(1+\frac{\gamma-1}{2}Ma_{\mathrm{th}}^2\right)^{\frac{\gamma}{\gamma-1}} = p_{\mathrm{th}}\left(\frac{\gamma+1}{2}\right)^{\frac{\gamma}{\gamma-1}} \tag{1}$$

A high speed camera is put against the exit of the RDE to capture the video data of the rotating detonation waves in the chamber. The whole RDE is bedded on the moving part of the thrust stand, and the thrust is measure by a thrust transducer. In our experiments, we used gaseous methane (CH_4) as fuel and gaseous oxygen (O_2) as oxidizer. The feeding mass flow rate is measured by two Coriolis flowmeters in the feeding system. The total mass flow rate varies between 100-300g/s, and the range of equivalence ratio varies between 0.5-1.2.

3 Result and discussion

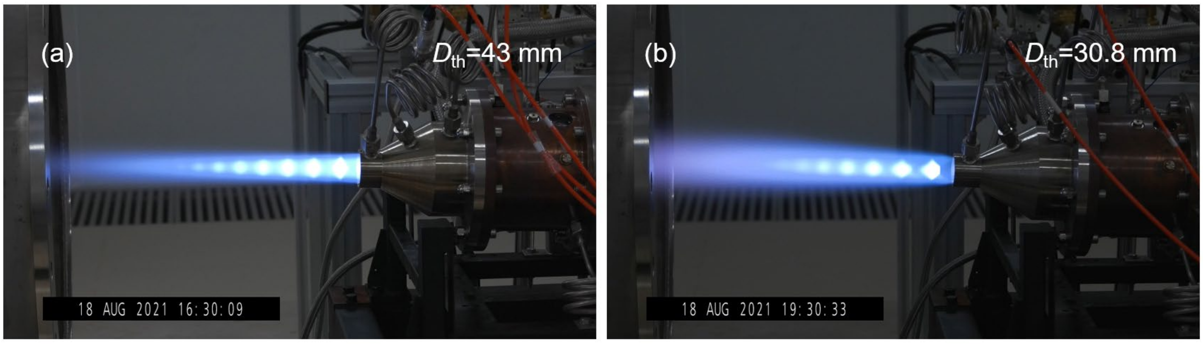

Figure 2: An picture of the hollow RDE with Laval nozzle of which (a) the throat diameter is 43 mm; (b) the throat diameter is 30.8 mm.

As expected, we obtain steady rotating detonation waves and choked operating state in our experiments of the facility descripted above. Figure 2 shows the typical pictures during the operation of the hollow RDE. The Mach disks is very clear during the operation.

The average test measurements are captured during the stable duration of each hot-fire test, including time averaged pressure of fuel and oxidizer plenum, the measurements of CTAPs, the trust and the mass flow rate. As is known, the directly measured chamber pressure of the combustion chamber of traditional rocket engine is usually regarded as the total pressure of the chamber, under the assumption that the flow in the chamber is very weak, but whether it is the same with RDE chamber is unknown. So first we compared the total pressure obtained from throat pressure p_{th} and the pressure at the end of the chamber and at the entrance of the Laval nozzle, and it is found that the pressure obtained from two methods are almost the same, so it is reasonable to adopt the p_3 as the total pressure of the chamber.

The specific impulse is a very important parameter for rocket designing. As is known, the specific impulse would increase as the pressure ratio of chamber to environment. Quite a lot of researchers[11] have observed the same trend in RDE with an annular chamber, but it is still unknown to what extent can be the trend of the hollow RDE consistent with the previous researches. Here we investigated the specific impulse and the chamber pressure of the hollow rocket RDE. The result is shown in Figure 3.

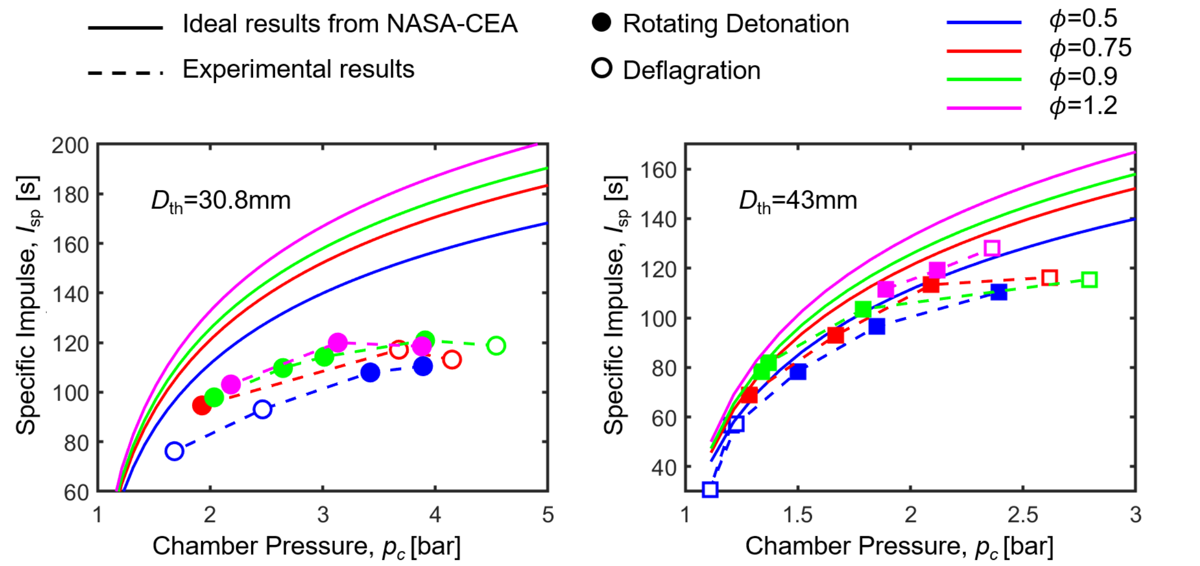

Figure 3: The specific impulse I_{sp} versus combustion chamber pressure p_c.

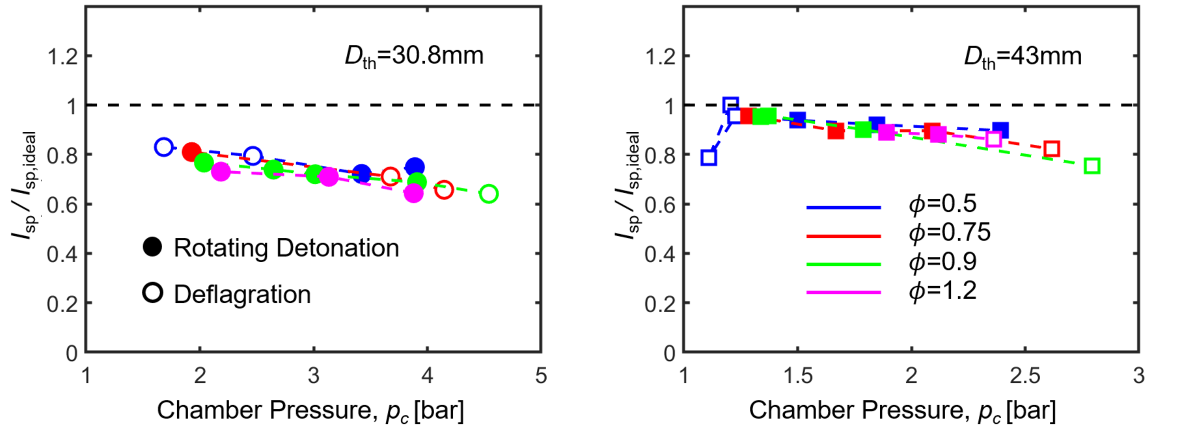

Figure 4: The experiment-pressure-based normalized specific impulse $I_{sp,ideal}$ versus combustion chamber pressure p_c.

The dashed line represents the measured specific impulse I_{sp}, and the solid line represents the ideal specific impulse $I_{sp,ideal}$ calculated from NASA-CEA[12] code. The back pressure was set to be 1 atm. We normalized the measured specific impulse by the ideal specific impulse $I_{sp,ideal}$, and the result is shown in Figure 4. The solid markers indicate operating conditions that successfully produced rotating detonation waves, meanwhile the unfulfilled markers indicate the operating conditions that failed to produce detonation and under which the engine stably operated in deflagration mode. The different colors represent different equivalent ratios ϕ. It is shown that the specific impulse I_{sp} does increase as the chamber pressure p_c increases in both configurations, and also increases as the equivalent ratio increases between 0.5-1.2. The specific impulse is lower than the ideal value and the ratio of the measured value I_{sp} to ideal value $I_{sp,ideal}$ distributes between 0.6-1. Apparently, the I_{sp} of the nozzle with 30.8 mm throat diameter (Nozzle.1) is lower overall than the nozzle with 43 mm throat diameter (Nozzle.2). When the geometry configuration of these two nozzles are taken into consideration, the distraction ratio of Nozzl.1 is a little bit larger than Nozzle 2, which would cause an over expansion to greater degree. This might cause some extra deficit of the specific impulse of the combustor.

Characteristic velocity c^* is only a function of propellant characteristics and combustion chamber properties, independent of nozzle characteristics[13]. The characteristic velocity c^* is given by

$$c^* = \frac{p_c A_{\text{th}}}{\dot{m}} \tag{2}$$

In our study, we calculate the ideal characteristic velocity c^*_{ideal} using the iteration method Stechmann[14] came up with. And then we normalize the measured characteristic velocity c^* by the ideal value c^*_{ideal}, then we get the c^* efficiency η_{c^*} (Figure 5)

$$\eta_{c^*} = \frac{c^*_{\text{ex}}}{c^*_{\text{ideal}}} \tag{3}$$

which can be used to express the degree of completion of chemical energy releases in the generation of high-temperature, high-pressure gases in combustion chambers. It should be noted that the ideal value c^*_{ideal} is calculated under choked condition in NASA-CEA, so only the values distributed on the right side of the choked lines are credible. It is shown that the c^* efficiency η_{c^*} is all beneath the unit value. The values of Nozzle.1 distribute around 0.7, while the values of Nozzle.2 distribute around 0.8, which are a bit higher than Nozzle 1. The cause for this phenomenon still needs further investigation, but it can be inferred that some mixing issues caused by the coupling of combustion chamber and the propellant plenums. It can be seen that a lower equivalence ratio tends to lead to a higher c^* efficiency. This might indicate that the mixing property is not as ideal as we expected, because the existence of more oxidizer seems to lead to a better mixing and therefore higher c^* efficiency, so it is necessary to change our injecting structure and investigate the effects of the injecting structure on the hollow RDE.

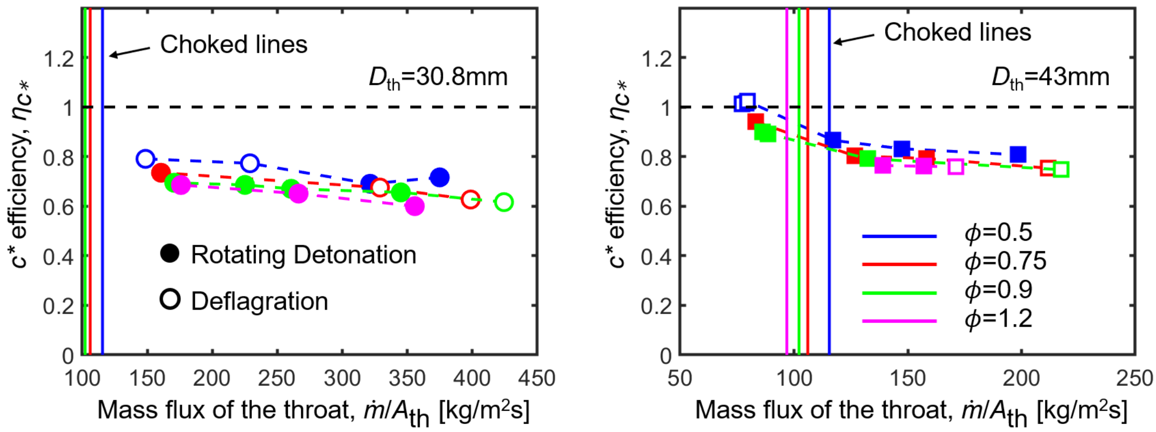

Figure 5: The c^* efficiency η_{c^*} versus mass flux of the throat $\dot{m}/A_{\text{th}}$.

In addition, we noted an interesting phenomenon that it seems that there is a trend that the performance of detonation is a little bit better than that of deflagration under the same condition, both in normalized specific impulse and the c^* efficiency. This encouraging conclusion still needs further systematic and detailed research, which has already been on going in our laboratory.

4 Conclusions

A preliminary study of the propulsive performance of the hollow RDE with Laval Nozzles of two configurations has been carried out. The Laval nozzles has a throat of 30.8 mm and 43 mm in diameter respectively which assures that the burned exhaust gas would be choked under most test conditions. We calculated the specific impulse I_{sp} of the hollow RDE. It is shown that the specific impulse was 0.6-1.0 that of the ideal value. It is found that the specific impulse of the hollow RDE increases as the chamber pressure increases, which is consistent with previous studies. There is also a trend that the specific impulse also increases as the equivalence ratio increases from 0.5 to 1.2. Besides, we also investigated the $c*$ efficiency η_{c*}. The results show that the $c*$ efficiency of the nozzle with throat diameter of 43 mm is a bit higher than that of 30.8 mm, which might be due to the injecting structure and the coupling of the combustion chamber and the propellant plenum and need further research.

Moreover, an encouraging phenomenon was also noted that the performance of detonation is a little bit higher than that of deflagration under the same test condition. Further study is in progress to verify this results in our laboratory.

References

[1] B. Voitsekhovskii, "Stationary Spin Detonation," *Sov. J. Appl. Mech. Tech. Phys.*, vol. 3, no. 3, pp. 157–164, 1960.

[2] J. A. Nicholls, H. R. Wilkinson, and R. B. Morrison, "Intermittent detonation as a thrust-producing mechanism," *Jet Propuls.*, vol. 27, no. 5, pp. 534–541, 1957.

[3] F. A. Bykovskii and V. V. Mitrofanov, "Detonation combustion of a gas mixture in a cylindrical chamber," *Combust. Explos. Shock Waves*, vol. 16, no. 5, pp. 570–578, Sep. 1980.

[4] X.-M. Tang, J.-P. Wang, and Y.-T. Shao, "Three-dimensional numerical investigations of the rotating detonation engine with a hollow combustor," *Combust. Flame*, vol. 162, no. 4, pp. 997–1008, Apr. 2015.

[5] W. Lin, J. Zhou, S. Liu, and Z. Lin, "An experimental study on CH4/O2 continuously rotating detonation wave in a hollow combustion chamber," *Exp. Therm. Fluid Sci.*, vol. 62, pp. 122–130, Apr. 2015.

[6] V. Anand, A. C. St. George, and E. J. Gutmark, "Hollow Rotating Detonation Combustor," presented at the 54th AIAA Aerospace Sciences Meeting, San Diego, California, USA, Jan. 2016.

[7] H. Zhang, W. Liu, and S. Liu, "Experimental investigations on H2/air rotating detonation wave in the hollow chamber with Laval nozzle," *Int. J. Hydrog. Energy*, vol. 42, no. 5, pp. 3363–3370, Feb. 2017.

[8] A. Kawasaki *et al.*, "Critical condition of inner cylinder radius for sustaining rotating detonation waves in rotating detonation engine thruster," *Proc. Combust. Inst.*, vol. 37, no. 3, pp. 3461–3469, Jan. 2019.

[9] K. Goto *et al.*, "Cylindrical Rotating Detonation Engine Cooling by Means of Propellant Injection," presented at the AIAA Propulsion and Energy 2020 Forum, VIRTUAL EVENT, Aug. 2020.

[10] R. Yokoo *et al.*, "Propulsion Performance of Cylindrical Rotating Detonation Engine," *AIAA J.*, vol. 58, no. 12, pp. 5107–5116, Dec. 2020.

[11] K. Goto *et al.*, "Propulsive Performance and Heating Environment of Rotating Detonation Engine with Various Nozzles," *J. Propuls. Power*, vol. 35, no. 1, pp. 213–223, Jan. 2019.

[12] B. J. McBride and S. Gordon, "Computer Program for Calculation of Complex Chemical Equilibrium Compositions and Applications II. Users Manual and Program Description." Jun. 01, 1996.

[13] G. P. Sutton and O. Biblarz, *Rocket Propulsion Elements*. John Wiley & Sons, 2016.

[14] D. P. Stechmann, "Experimental Study of High-Pressure Rotating Detonation Combustion in Rocket Environments," Ph.D., Purdue University, Ann Arbor, 2017.